Arthritis & Rheumatology
Vol. 0, No. 0, Month 2025, pp 1–12
DOI 10.1002/art.43273

American College of Rheumatology
Empowering Rheumatology Professionals

Loss of Tripartite Motif–Containing Protein 21 and UVB-Induced Systemic Inflammation by Regulating DNA-Sensing Pathways

Gantsetseg Tumurkhuu,[1] Graziela Perri,[1] Richard Moore,[1] Lihong Huo,[1] Arati Naveen Kumar,[1] Richard Ainsworth,[1] Trinitee Oliver,[1] Gabriela De Los Santos,[1] David Gibb,[1] Jessica Carriere,[1] Jeong Min Yu,[1] Rachel Abuav,[1] Lindsy Forbess,[1] Daniel J. Wallace,[2] Mariko Ishimori,[2] Wonwoo Shon,[1] Christian Stehlik,[1] and Caroline A. Jefferies[1,3]

Objective. Patients with systemic lupus erythematosus (SLE) experience photosensitivity, with exposure to UVB light driving lupus flares and triggering symptoms like joint pain, fatigue, and cutaneous lesions. Although the mechanism(s) linking UVB exposure to systemic effects are unclear, type I interferons (IFNs) are known to play a role. Our previous work has shown that TRIM21, an autoantigen in SLE, functions as a negative regulator on the pathways driving IFN expression. Here we explore how TRIM21 functions to regulate both local and systemic inflammation following UVB exposure and how altered expression may drive cutaneous inflammation and photosensitivity in SLE.

Methods. Wild-type (WT; C57BL/6) and *Trim21*$^{-/-}$ mice were irradiated with UVB (100 mJ/cm^2) on the shaved dorsal region on consecutive days for 1 and 3 weeks, and UVB-induced local cutaneous manifestations and systemic inflammation in blood, spleen, and kidney were examined by messenger RNA expression of inflammatory and type I IFN response genes, histology, and flow cytometry. Mechanistic studies were performed in bone marrow–derived macrophages (BMDMs) and murine dermal fibroblasts (MDFs) from WT and *Trim21*$^{-/-}$ mice and *TRIM21*$^{-/-}$ THP-1 cells.

Results. Infiltration of inflammatory cells and induction of type I IFN developed in UVB-exposed areas in both sets of mice. Most notably after UVB exposure, we observed splenomegaly and enhanced expression of IFN-stimulated genes in the blood and spleen of *Trim21*$^{-/-}$ mice. Inflammatory chemokines CXCL10 and CXCL12 were also detected at significantly higher levels in serum of *Trim21*$^{-/-}$ mice after UVB exposure. *Trim21*$^{-/-}$ mice exposed to UVB also demonstrated enhanced total IgG levels in serum accompanied by increased skin and kidney deposition of IgG and increased glomerular cellularity and size. To determine the mechanism, we assessed UVB- and cyclic GMP-AMP–dependent *Ifnb1* expression in *Trim21*$^{-/-}$ BMDMs and MDFs, noting increased responses compared with WT cells. This effect was lost in BMDMs from *Trim21/Sting1* double knockout mice and skin explants, in keeping with the ability of TRIM21 to regulate cytoplasmic DNA sensing. In keeping with previous reports, we found that degradation of both DDX41 and STING levels were affected in stimulated *Trim21*$^{-/-}$ BMDMs.

Conclusion. Taken together, our results indicate that TRIM21 protects against IFN induction at both local and systemic levels by restricting STING signaling.

INTRODUCTION

Abnormal responses to UVB light or photosensitivity are experienced by approximately two-thirds of patients with systemic lupus erythematosus (SLE), with sun exposure triggering local skin inflammation, increased systemic activity (flare), or both.[1] The mechanisms that predispose patients to develop systemic disease flares in response to sun exposure are unclear and are an important gap in our knowledge regarding the pathophysiology of this disease. Elevated type I interferon (IFNα, β, and κ) and IFN-stimulated genes (ISGs) are the most common immunologic abnormality in SLE and are associated with disease severity and organ involvement, including cutaneous involvement.[2,3] Photosensitivity to UVB is a well-known trigger of both

Supported by the National Institute of Arthritis and Musculoskeletal and Skin Diseases, NIH (grant R56-AR-078279-01A1), Center for Research in Women's Health Science at Cedars-Sinai Medical Center (CSMC) with support from Donner Foundation and CSMC Academic Affairs, and Leon Fine Translational Science

localized cutaneous disease (cutaneous lupus erythematosus [CLE]) and systemic disease. In cutaneous manifestations of SLE, high levels of type I IFNs are detected in both lesional and nonlesional skin and correlate with systemic ISG expression.[4] UVB exposure has multiple effects on keratinocytes, the first line of defense against exposure, including IFN induction.[2,5] However, the molecular links between UVB photosensitivity and the development of systemic disease are unknown.

UVB exposure triggers several biologic pathways in the skin, including DNA damage, DNA repair, cell death, and release of self-nucleic acids. Self-RNA and DNA (mitochondrial and nucleic) act as potent damage-associated molecular patterns and are detected by cytosolic nucleic acid sensors[3,6–10] such as cGAS and DDX41.[11–13] cGAS, once it binds double-stranded DNA (dsDNA), synthesizes the cyclic dinucleotide cyclic GMP-AMP (cGAMP), which acts as a second messenger in the cell, binding and activating the adapter protein STING to drive IFNβ induction.[14–17] DDX41 can also bind cGAMP and STING and drive IFNβ expression.[11,12] Recent work has clearly implicated cGAS and STING in UVB-mediated IFN expression in the skin of C57BL/6 mice, with the absence of STING or cGAS preventing IFN induction in the skin following UVB exposure.[18,19]

TRIM21, otherwise known as Ro52, is a common autoantigen associated with cutaneous SLE and is commonly upregulated in photo-provoked skin.[20] Moreover, anti-Ro52/TRIM21 antibodies accumulate in CLE skin and exacerbate local inflammatory responses. As an E3 ubiquitin ligase, TRIM21 negatively regulates type I IFN induction downstream of RNA- and DNA-sensing pathways by ubiquitinating and targeting DDX41 and the transcription factors IFN regulatory factor (IRF) 3, 5, and 7 for proteasomal degradation.[21–29] In doing so, TRIM21 limits the IFN response and prevents autoimmune disease. *Trim21*-deficient mice develop splenomegaly and a lupus-like systemic disease as a result of enhanced toll-like receptor 7– and 9–induced IFN induction, driven by increased levels of IRF3, 5, and 7.[25] Importantly *Trim21*$^{-/-}$ mice exhibit skin lesions that are provoked by DNA damage, suggesting *Trim21* may play an important role in skin involvement in SLE.[25]

In this study we explored the potential that loss of *Trim21* might exacerbate UVB-induced skin and systemic inflammation. We found *Trim21* deficiency results in enhanced local and systemic inflammation and ISG expression of UVB-exposed mice. In addition to increased DDX41 stability, we observed *Trim21*$^{-/-}$ cells fail to degrade STING after engaging the cGAS/STING pathway, resulting in up-regulated type I IFN and ISGs. Our findings show that TRIM21 is an important regulator of systemic IFN responses following UVB challenge in the skin and suggest that loss of TRIM21 expression or activity in the skin of patients with SLE with cutaneous involvement may enhance UVB-induced systemic involvement.

MATERIALS AND METHODS

Mice. *Trim21*$^{GFP/GFP}$ mice (*Trim21*$^{-/-}$) were a gift from the Dr Wahren-Herlenius laboratory.[25] C57BL/6 and *Sting*$^{gt/gt}$ mice were purchased from The Jackson Laboratory. Mice were propagated and maintained in the animal facility at the Department of Comparative Medicine (Davis Building) of Cedars-Sinai Medical Center. Animals were between 8 and 12 weeks old at the time of experimentation. All experiment procedures were approved by institutional Animal Care and Use Committee.

UVB irradiation regimen. Eight-week-old wild-type (WT) and *Trim21*$^{-/-}$ mice were shaved dorsally before UVB exposure. Mice were allowed to move freely in their cage during UVB exposure, and mice were treated with/without UVB 100 mJ/cm^2 for 1 or 3 weeks.

Isolation of tissue for flow cytometry. Skin lesions, spleen, kidney, and blood were harvested following final UVB exposure. Single-cell suspensions were incubated in blocking buffer (2% fetal bovine serum and 1% anti-Fc Block [BioLegend] in phosphate-buffered saline [PBS]) for 30 minutes, followed by staining with mouse-specific fluorescent antibodies CD45 Alexa Fluor 700 (clone:30-F11), CD3 PE/Cy7 (clone 145-2C11), CD4 APC/Cy7 (clone GK1.5), CD11b Pacific Blue (clone M1/70), Ly6G APC (clone 1A8), and CCR2 PE (clone SA203G11), all purchased from BioLegend; and Siglec1 BV421 (clone 7-239) (BD Bioscience) for 45 minutes. All samples were processed using an SA3800 flow cytometer (Sony), and the data were analyzed with FlowJo VX.0.7 software (Tree Star).

Analysis of IgG and anti-dsDNA IgG antibody serum levels. Serum was collected after UVB treatment. Total IgG and

Award, CSMC, to Dr Jefferies; the National Institute of Allergy and Infectious Disease, NIH (grant R01-AI-134030), to Dr Stehlik; and the National Heart, Lung, and Blood Institute, NIH (grant R03-HL-1586) to Dr Gibb.

[1]Gantsetseg Tumurkhuu, PhD, Graziela Perri, PhD, Richard Moore, MS, Lihong Huo, PhD, Arati Naveen Kumar, MA, Richard Ainsworth, PhD, Trinitee Oliver, XX, Gabriela De Los Santos, MD, David Gibb, PhD, Jessica Carriere, PhD, Jeong Min Yu, MD, Rachel Abuav, MD, Lindsy Forbess, MD, Wonwoo Shon, MD, Christian Stehlik, PhD, Caroline A. Jefferies, PhD: Cedars-Sinai Medical Center, Los Angeles, California; [2]Daniel J. Wallace, MD, Mariko Ishimori, MD: Cedars-Sinai Medical Center and University of California, Los Angeles; [3]Caroline A. Jefferies, PhD: Kao Autoimmunity Institute, Cedars-Sinai Medical Center, Los Angeles.

Drs Tumurkhuu and Perri contributed equally to this work.

Additional supplementary information cited in this article can be found online in the Supporting Information section (https://acrjournals.onlinelibrary.wiley.com/doi/10.1002/art.43273).

Author disclosures are available online at https://onlinelibrary.wiley.com/doi/10.1002/art.43273

Address correspondence via email to Caroline A. Jefferies, PhD, at caroline.jefferies@cshs.org.

Submitted for publication April 23, 2024; accepted in revised form May 19, 2025.

anti-dsDNA IgG antibody levels were analyzed via enzyme-linked immunosorbent assay kits (6320 and 5120, Alpha Diagnostic).

Histopathology, immunohistochemistry, and immunofluorescence. Tissue samples were perfused with PBS and immersed in 10% buffered formalin for 48 hours at 4°C and paraffin embedded and stained using hematoxylin and eosin or antibodies as appropriate. For kidney analysis, glomerular size was determined by calculating the radius (r) of each glomerulus in ImageJ software, and the area was calculated from at least 20 glomeruli from each different group. Glomerular cellularity was determined by counting the total number of nuclei in each glomerulus by ImageJ software. Images were taken on a Zeiss Axio and Echo Microscopy. IgG and CXCL10 intensities were quantified using ImageJ.

Patients and healthy controls. This study was approved by the institutional review board at Cedars-Sinai Medical Center and in line with the principles of the Declaration of Helsinki. Participants were recruited from the lupus clinic at Cedars-Sinai Medical Center. Blood samples were collected from all patients and age-matched controls using PAXgene Blood RNA tubes. The SLE Disease Activity Index (SLEDAI) score was determined for each patient at the time of the blood draw. All participants provided informed written consent, and the study received prior approval from the relevant institutional ethics review boards. Patient demographics are given in Supplemental Table 1.

PAXgene RNA isolation and RNA sequencing. RNA was isolated using the PAXgene Blood RNA kit according to the manufacturer's guidelines (PreAnalytiX). Stranded RNA sequencing (RNA-Seq) library construction was performed using the xGen Broad-Range RNA Library Prep Kit (Integrated DNA Technologies). Multiplexed libraries were sequenced on a NovaSeq 6000 (Illumina) using 75-bp single-end sequencing. On average, approximately 50 million reads were generated from each sample.

Bioinformatics and data analysis. Raw reads obtained from RNA-Seq were aligned to the transcriptome using STAR (version 2.5.0)/RSEM (version 1.2.25) with default parameters, using a custom mouse GRCm39 transcriptome reference downloaded from https://www.gencodegenes.org. Expression counts for each gene in all samples were normalized by a modified trimmed mean of the M-values normalization method and the unsupervised principal component analysis was performed with DESeq2 Bioconductor package version 1.42.0 in R version 4.3. The Benjamini and Hochberg procedure was applied to adjust for multiple hypothesis testing, and differential expression gene candidates were selected with a false discovery rate <0.05. For functional enrichment analysis across sample groups, we conducted genes enrichment analysis using the R packages "clusterProfiler" v4.10.0[30] and "pathfindR" v2.3.1.[31]

Single-cell RNA-seq data reprocessing. Preprocessed single-cell RNA-seq data from lesional (L)/nonlesional (NL) lupus skin and healthy normal (H) skin[4] (GSE186476) were analyzed using the R package "Seurat" (v4.3.0).[32] Fibroblasts were subset and the expression of TRIM21 visualized using the function *VlnPlot*, split by disease state. Differential expression analysis between disease states was conducted using the *FindMarkers* function with default settings.

Isolation, culture, and stimulation of cells and tissue. Bone marrow–derived macrophages (BMDMs) were cultured as previously described.[33] Murine dermal fibroblasts (MDFs) and skin explants were cultured as previously described.[34,35] Before stimulation, MDFs and skin explants were starved in 2% fetal bovine serum–supplemented medium for 24 hours before exposure to 50, 100, or 500 mJ/cm^2 UVB.

Fifty nanometers of immunostimulatory dsDNA (ISD) were transfected into BMDMs or THP-1 cells with Lipofectamine (L3000008, ThermoFisher Scientific) for 1, 2, 4, or 8 hours. The 2'-3-cGAMP (tlrl-nacga23-1, InvivoGen) was added at 10 μg/mL with or without 4 μM H151 (inh-h151, InvivoGen) to cell supernatant (added 30 minutes before stimulation) for 1, 2, 4, or 8 hours.

Generation of *TRIM21*$^{-/-}$ and THP-1 cells and *TRIM21* knock-in of *TRIM21*$^{-/-}$ THP-1 cells. *TRIM21*$^{-/-}$ THP-1 cells were generated using CRISPR/Cas9 targeting. Two guide RNAs (gRNAs) were designed to target hTRIM21 Exon 2: gRNA#1: ATGCTCACAGGCTCCACGAA (Exon2 ORF bp67-86); gRNA#2: ATGTTGGCTAGCTGTCGATT (Exon2 ORF bp196-215) and cloned into lentiCRISPRv1 (Addgene, plasmid 49535). After lentiviral transduction using lentiCRISPRv1 as a control as described below, clonal populations were screened by polymerase chain reaction (PCR) amplification and sequencing of the targeted genomic sequence using the following primers: hTrim21gRNA1-Fwd (GTCTCCACACTGCTGTTTAACG) and hTrim21gRNA2-Rev (TTCCCATCTTTCTCACAGAACA).

To restore *TRIM21* expression into *TRIM21*$^{-/-}$ THP-1 cells, hTRIM21 full-length coding DNA sequence with N-terminal Myc and enhanced green fluorescent protein (eGFP) was cloned into pLEX-MCS and transfected into HEK293T-Lenti cells (Clontech 632180) along with pMD.2G and psPAX2 (Addgene, plasmids 12259 and 12260) to generate lentiviral particles. Forty-eight hours after transfection, lentiviral suspensions were harvested, passed through 0.45-μm filters and mixed with 106 TRIM21KO THP-1 cells in the presence of 0.5 μg/mL of polybrene. Cells were centrifuged at 1,800 revolutions per minute for 50 min at 32°C. After overnight incubation at 37°C, the medium was changed, and EGFP$^+$ cells were sorted 72 hours after infection.

Western blot and gene expression analysis. Cell lysates were separated by SDS-PAGE gel electrophoresis, transferred to polyvinylidene difluoride membranes, and analyzed

using the following antibodies: anti-DDX41 (Novus Bio), anti-IRF3 (clone D83B9, Cell Signaling Technology), anti-STING (Novus Bio), anti-TRIM21 (clone EPR20290, abcam), and anti–β-actin (Cell Signaling Technology). RNA was isolated using the TRI Reagent (Millipore Sigma). Following complementary DNA synthesis, reactions were run in triplicate on a StepOnePlus real-time PCR instrument (Applied Biosystems) using gene-specific primers. Ct values were standardized to the house-keeping gene *Rn18s* (mouse) or *RNA18SN* (human).

The following murine primer sequences were used:

Rn18s, 5′-GAGGGAGCCTGAGAAACGG-3′ (F) 5′-GTCGGGAGTGGGTAATTTGC-3′ (R);
Cxcl10, 5′-GCCGTCATTTTCTGCCTCAT-3′ (F) 5′-GCTTCCCTATGGCCCTCATT-3′ (R);
Ifnb1, 5′-CAGCTCCAAGAAAGGACGAAC-3′(F) 5′-GGCAGTGTAACTCTTCTGCAT-3′ (R); and
Isg15, 5′-GGTGTCCGTGACTAACTCCAT-3′ (F) 5′-TGGAAAGGGTAAGACCGTCCT-3′ (R).

The following human primer sequences were used:

IFNB1, 5′-CTTGGATTCCTACAAAGAAGCAGC-3′(F); 5′-TCCTCCTTCTGGAACTGCTGCA-3′(R) and
TRIM21, 5′-TCAGAGCTAGATCGAAGGTGC-3′(F); 5′-ACTCACTCCTTTCCAGGACAAT-3′(R).

Statistics. All data are expressed as mean ± SD. Statistical differences were measured using either a Student's unpaired *t*-test or two-way analysis of variance (ANOVA) with Bonferroni post-hoc test when appropriate. Normality of data was assessed via a Shapiro-Wilk normality test. When the data analyzed were not distributed normally, we used the Mann-Whitney test or Kruskal-Wallis one-way ANOVA with the Dunn post-hoc test. Data analysis was performed using Prism software version 7.0a (GraphPad). A P value of <0.05 was considered statistically significant. P values <0.05 are significant, and asterisks in the figures represent the specific significant values. Data are available in GEO at https://www.ncbi.nlm.nih.gov/geo, reference number GSE265768.

RESULTS

Loss of TRIM21 accelerates UVB-induced cutaneous inflammation. UVB and UVC light drive type I IFN in keratinocytes, and both acute and repeated UVB exposure result in the upregulation of type I IFN and ISGs within the skin of mice.[36] Mice lacking TRIM21 develop severe dermatitis and systemic autoimmunity in response to chronic physical injury.[25] To assess whether TRIM21 plays a role in regulating the IFN response to chronic UVB exposure, we shaved *Trim21*$^{+/+}$ (WT) and *Trim21*$^{-/-}$ (knockout) C57BL/6 mice and exposed them to a low dose of UVB light on consecutive days over 3 weeks. Although both WT and *Trim21*$^{-/-}$ animals demonstrated similar levels of infiltrating CD45^{+} immune cells into the skin following chronic UVB exposure (Supplemental Figure 1A), CD11b^{+} cells were increased in UVB-exposed *Trim21*$^{-/-}$ skin (Figure 1A) and had higher levels of the ISG Siglec1 compared with WT CD11b^{+} cells (Figure 1B). In addition, IFNβ and the ISG *Cxcl10* were significantly up-regulated in *Trim21*-deficient skin tissue compared with WT (Figure 1C), with skin from *Trim21*-deficient animals showing increased IgG in the skin after UVB compared with WT, albeit not significantly (Figure 1D).

Loss of *Trim21* enhances the systemic inflammatory response to UVB. Circulating CCR2^{+} monocytes are up-regulated in response to UVB exposure and migrate to the UVB-exposed tissue to drive inflammation.[19] In line with this, we observed increased CD11b^{+}Ly6G^{+} circulating neutrophils and CD11b^{+}Ly6C^{+} inflammatory monocytes in UVB-exposed *Trim21*$^{-/-}$ mice compared with WT controls (Figure 2A). Importantly, circulating CCR2^{+}CD11b^{+} myeloid cells were increased compared with WT and expressed higher levels of Siglec1 (Figure 2B). In addition, *Trim21*$^{-/-}$ mice had higher circulating IgG compared with WT (Figure 2C), although no increase in anti-dsDNA IgG was observed following 3 weeks of UVB exposure (data not shown).

Acute UVB exposure induces inflammation of the spleen and kidney.[37] Because of this, we asked if TRIM21 protected against systemic inflammation caused by chronic UVB exposure. We observed enhanced splenomegaly in *Trim21*$^{-/-}$ mice compared with WT (Figure 3A), with higher total levels of CD11b^{+} cells in the spleens of *Trim21*$^{-/-}$ mice (Supplemental Figure 1B). In addition, although splenic levels of CD11b^{+}Ly6G^{+} cells increased in the spleens of all UVB-exposed mice, the expansion was significantly higher in spleens of UVB-exposed *Trim21*$^{-/-}$ mice compared with WT (Figure 3B). In keeping with enhanced IFN responses, CD11b^{+} splenic populations from *Trim21*$^{-/-}$ mice had increased expression of the ISG Siglec1 compared with WT mice (Figure 3C). In addition, expression of *Ifnb1* and *Mx1* were enhanced in the spleens of UVB-exposed *Trim21*$^{-/-}$ mice (Figure 3D). Noticeably, the percentage of CD4^{+} T cells in the spleen increased in the absence of *Trim21* (Figure 3E), with central memory CD4 T cells being more highly represented in the spleens of *Trim21*$^{-/-}$ mice compared with WT (Figure 3F). Differential gene expression analysis of splenocytes from UVB-exposed WT and *Trim21*$^{-/-}$ mice demonstrated increased expression of neutrophil-specific genes (*Mpo*, *Elane*, *Prtn*, and *Camp*) and DNA-damage and UV response genes (*Rad51*) in *Trim21*$^{-/-}$ splenocytes compared with WT (Supplemental Figure 2A). Pathway analysis of differentially expressed genes identified increased expression of genes associated with mitosis and cell cycle regulation and decreased expression of genes associated with T cell activation and signaling through the

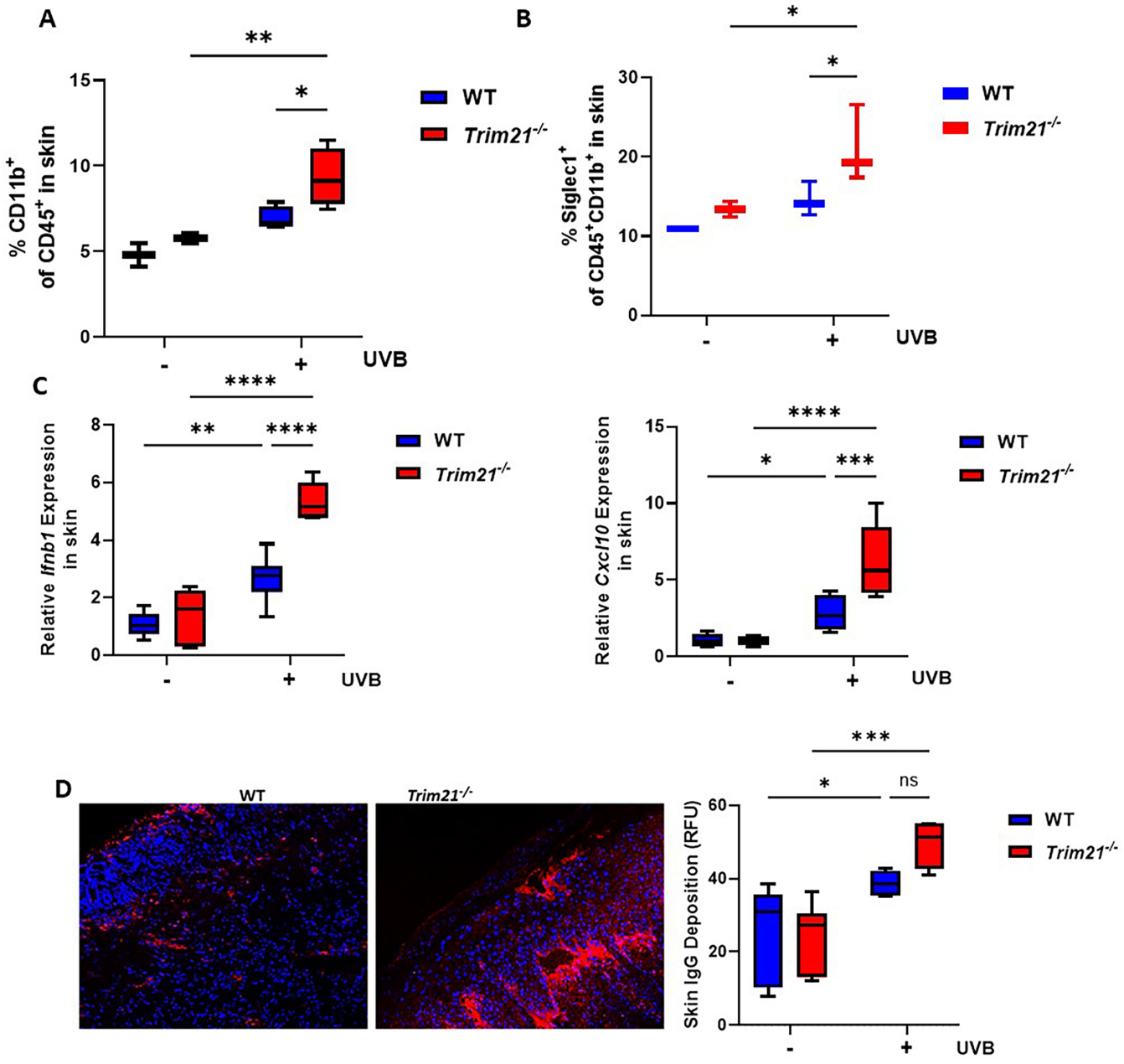

Figure 1. UVB skin irradiation induces a mixed local inflammatory response and higher cutaneous inflammation in *Trim21*$^{-/-}$ mice. Flow cytometry analysis following the final dose of the 3-week UVB treatment showing the percentage of infiltrating (n = 4 mice per group) (A) total myeloid cells in the skin and (B) Siglec1^{+} myeloid cells (CD11b^{+}CD45^{+}). (C) Cutaneous expression of *Ifnb1* and *Cxcl10* following 3-week UVB irradiation as determined by quantitative polymerase chain reaction. (D) IgG deposition in UVB-induced skin lesion with representative pictures and quantification analysis (four slides with two sections per group). All data represent mean ± SD and are representative of three independent experiments. Statistical significance was determined using two-way analysis of variance with the Fisher least significant difference test. In all cases, data representing WT and *Trim21*$^{-/-}$ mice are shown with blue and red bars, respectively. *P < 0.05; **P < 0.01; ***P < 0.001; ****P < 0.0001. ns, not significant; RFU, relative fluorescence unit; WT, wild-type.

interleukin-2 receptor, in keeping with our findings that central memory T cells were more highly represented in *Trim21*$^{-/-}$ splenocytes (Supplemental Figure 2B and C).

Increased kidney damage in *Trim21*$^{-/-}$ in response to UVB. We next asked if TRIM21 protected against kidney damage caused by chronic UVB exposure. Compared with WT, *Trim21*$^{-/-}$ kidneys displayed significantly increased glomerular size (Figure 4A and B) and cellularity (Figure 4A and C), suggesting increased immune infiltrate and inflammation. In accordance with TRIM21 regulating IFN, the levels of the ISG CXCL10 cytokine were significantly enhanced in *Trim21*$^{-/-}$ kidneys compared with WT (Figure 4A and

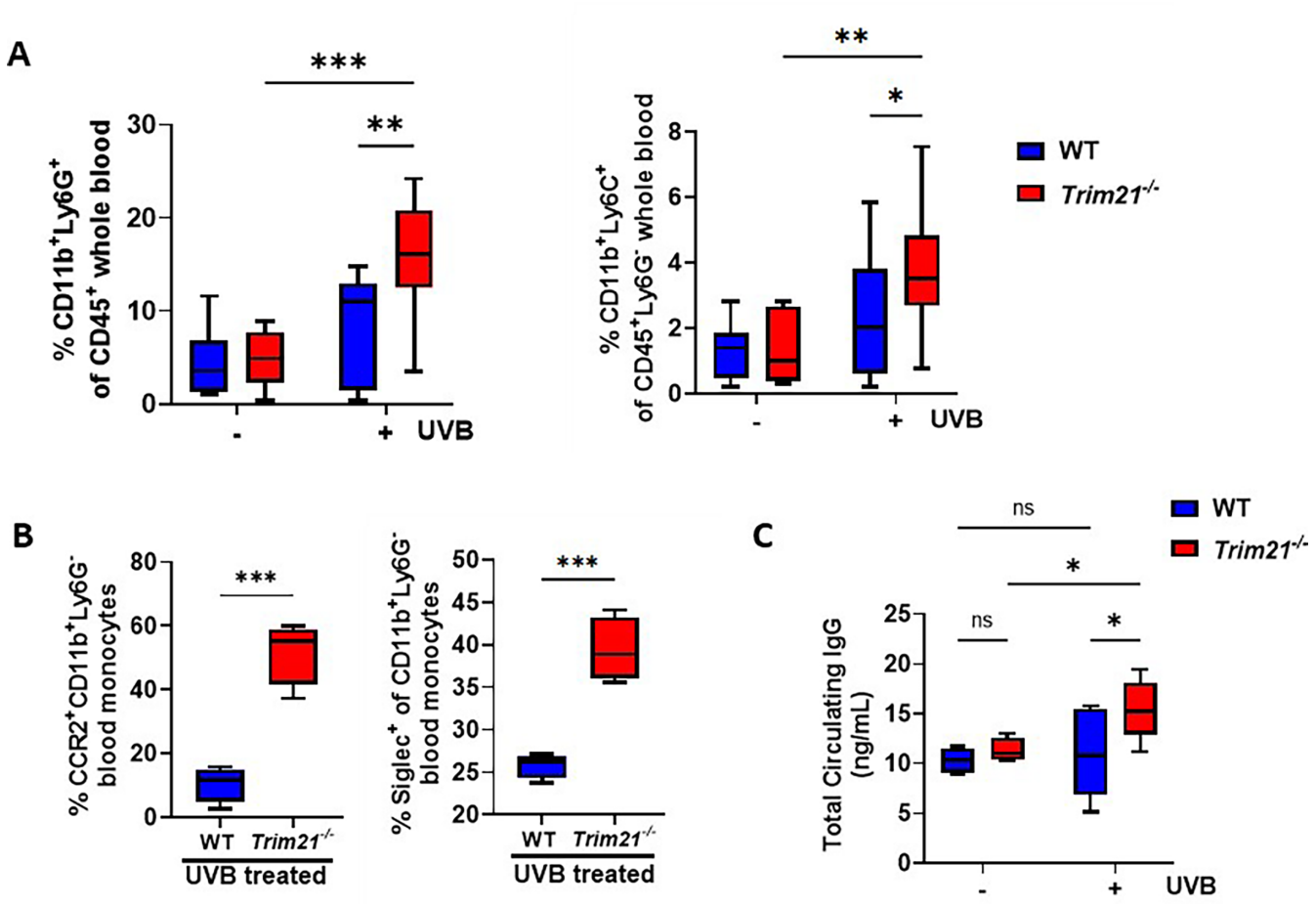

Figure 2. *Trim21* deficiency enhances systemic inflammation following UVB irradiation of the skin. Percentage of (A) neutrophils and inflammatory monocytes and of (B) CCR2$^+$ and Siglec1$^+$ CD11b$^+$Ly6G$^-$ cells from whole blood were analyzed via flow cytometry after the final dose of the 3-week UVB treatment (n = 4 mice per group). (C) Total circulating IgG was calculated via enzyme-linked immunosorbent assay. All data represent mean ± SD and are representative of three independent experiments. Statistical significance was determined using two-way analysis of variance with the Fisher least significant difference test or unpaired *t*-test. In all cases, data representing WT and *Trim21*$^{-/-}$ mice are shown with blue and red bars, respectively. *$P < 0.05$; **$P < 0.01$; ***$P < 0.001$. ns, not significant; WT, wild-type.

D). IgG deposition within the kidney is a common hallmark during SLE flares and, indeed, *Trim21*-deficient kidneys exhibited significantly increased IgG staining compared with WT (Figures 4A and E). Taken together, these results support a role for TRIM21 to restrain systemic inflammation in response to UVB exposure.

TRIM21 restricts the IFN-I response via STING signaling. The cGAS-STING pathway has recently been shown to regulate UVB-induced systemic responses in mice.[18,19,37] In addition, the DNA sensor DDX41 is a target for TRIM21-mediated ubiquitination and degradation. To assess the effect of TRIM21 deficiency on DDX41 and STING stability, we transfected WT and *Trim21*$^{-/-}$ BMDMs with ISD to activate cGAS upstream of STING, then analyzed DDX41 and STING stability by Western blotting. As previously published, DDX41 and STING were degraded in a time-dependent manner following ISD transfection of WT BMDMs, whereas both DDX41 and STING were stabilized in *Trim21*$^{-/-}$ BMDMs (Figure 5A), in addition to THP1 cells deficient in *TRIM21* compared with *TRIM21*-deficient THP-1 cells stably reconstituted with *Myc-EGFP-TRIM21* (Supplemental Figure 3A and B). This was accompanied by enhanced *Ifnb1/IFNB1* expression following activation of the cGAS-STING pathway (Figure 5B, Supplemental Figure 3C). Importantly, functional deletion of *Sting* by crossing *Trim21*$^{-/-}$ with *Sting Golden ticket (Gt)* mice, which harbor a single nucleotide variant (T596A) of *Sting* that functions as a null allele (*Trim21*$^{-/-}$*Sting*$^{gt/gt}$ BMDMs),[38] reversed the enhanced *Ifnb1* expression observed in the *Trim21*$^{-/-}$ BMDMs in response to ISD (Figure 5B). Similar results were observed in response to cGAMP stimulation of using *Trim21*$^{-/-}$*Sting*$^{gt/gt}$ BMDMs or using H151 (a specific STING inhibitor[39]) in *Trim21*$^{-/-}$ deficient BMDMs (Supplemental Figure 4A and B).

UVB-treated *Trim21*$^{-/-}$ MDFs showed enhanced *Ifnb1* expression compared with WT MDFs, which was inhibited by H151 (Supplemental Figure 4C). Similarly, UVB-irradiated skin

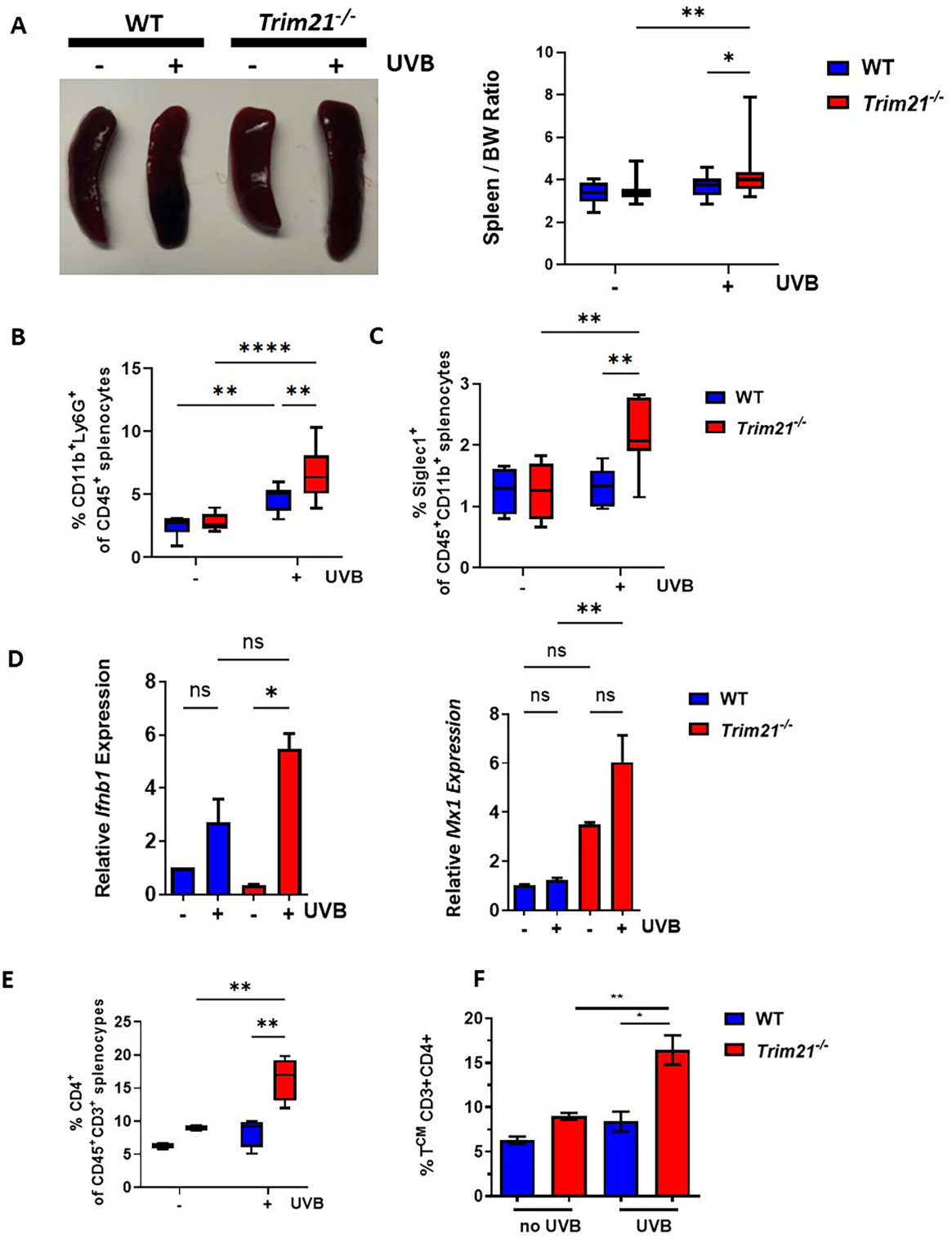

Figure 3. Splenic inflammation induced by chronic UVB irradiation is restrained by TRIM21. Following the final dose of the 3-week UVB treatment, (A) splenomegaly was measured by weight, comparing spleen weight with the BW of each mouse. Percentages of splenic (B) neutrophil cells and (C) Siglec1$^+$ CD11b$^+$ cells were analyzed via flow cytometry. (D) Splenocyte expression of *Ifnb1* and *Mx1* following 3-week UVB irradiation as determined by quantitative polymerase chain reaction. Percentages of splenic (E) CD4$^+$ T cells and (F) central memory T cells were analyzed via flow cytometry. All data represent mean ± SD and are representative of three independent experiments (n = 4 mice per group). Statistical significance was determined using two-way analysis of variance with the Fisher least significant difference test. In all cases, data representing WT and *Trim21*$^{-/-}$ mice are shown with blue and red bars, respectively. *$P < 0.05$; **$P < 0.01$; ***$P < 0.001$; ****$P < 0.0001$. BW, body weight; ns, not significant; WT, wild-type.

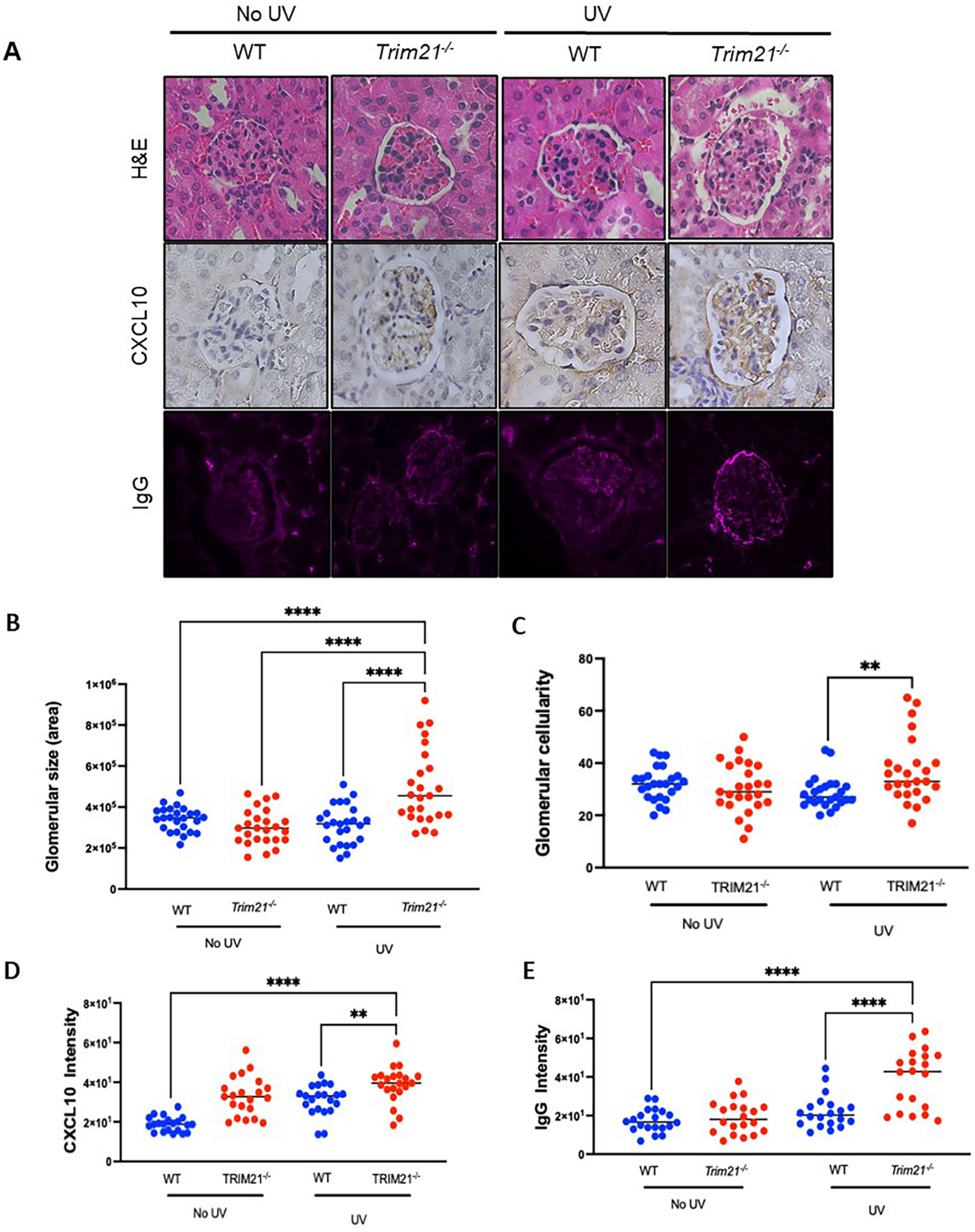

Figure 4. Skin exposure to UVB light induces kidney damage inflammation in *Trim21*$^{-/-}$ mice. (A) Representative images in the kidney tissues of C57BL/6 mice WT and *Trim21*$^{-/-}$ (no UV or UV) staining for H&E, CXCL10, and IgG (four slides with two sections per group). (B) Glomerular size was quantified on at least 20 glomeruli from four different mice group using Image J. (C) Glomerular cellularity was determined by counting the total nuclear cells in each group/glomerulus using Image J. (D) CXCL10 and (E) IgG staining intensity was measured using Image J. Images were taken at 40× (Echo Microscope). All data represent mean ± SD (n = 4 mice per group). Statistical significance was determined using one-way analysis of variance. In all cases, data representing WT and *Trim21*$^{-/-}$ mice are shown with blue and red dots, respectively. $^{**}P < 0.01$; $^{****}P < 0.0001$. H&E, hematoxylin and eosin staining; WT, wild-type.

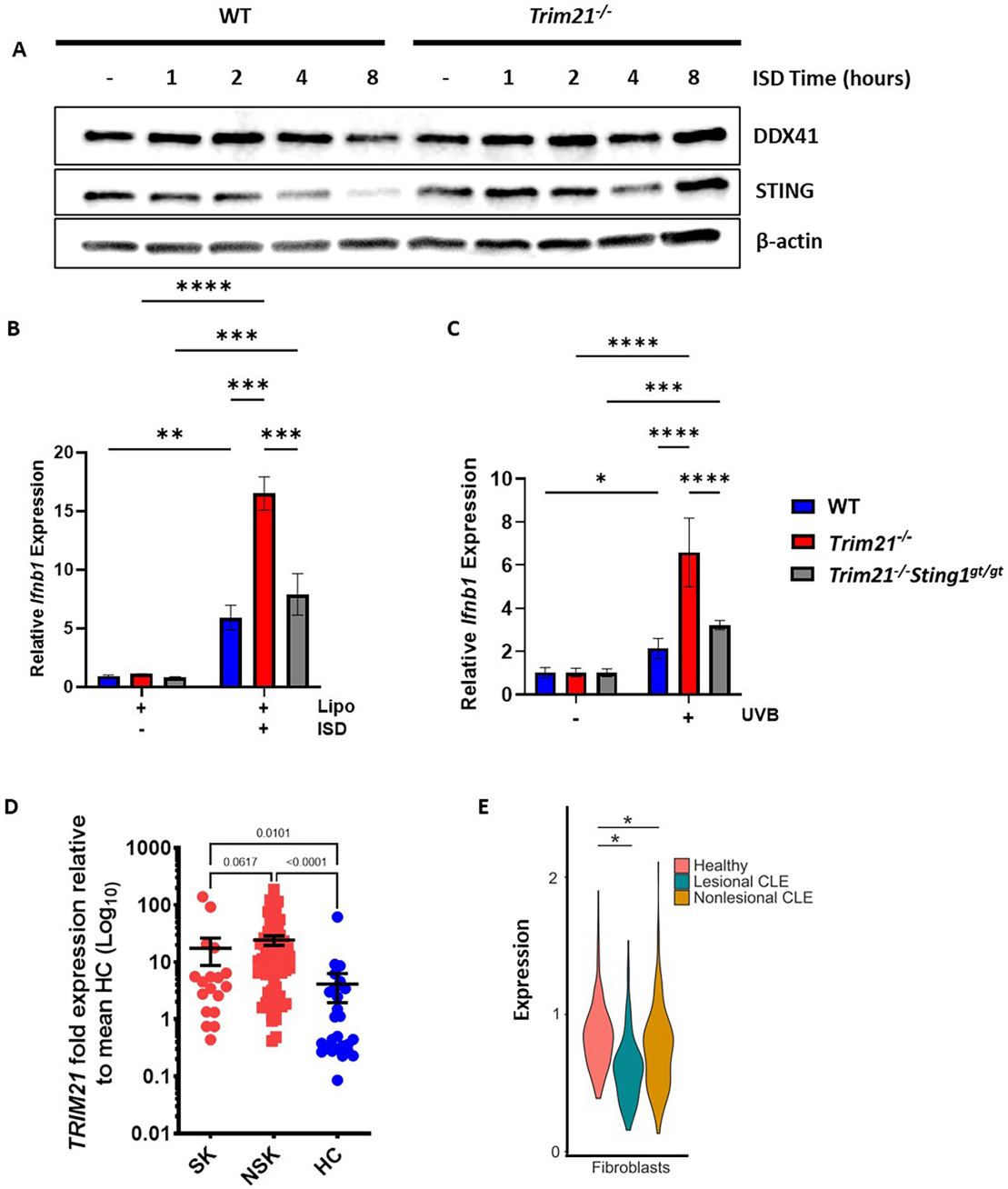

Figure 5. TRIM21 negatively regulates STING-dependent inflammation in response to UVB and cGAS-STING activation. (A) Bone marrow–derived macrophages from WT or *Trim21*$^{-/-}$ mice were transfected with ISD for the designated time, and protein levels of DDX41, STING, and β-actin were visualized via Western blotting. Images shown are representative of n = 3. (B) WT, *Trim21*$^{-/-}$, and *Trim21*$^{-/-}$*Sting*$^{gt/gt}$ bone marrow–derived macrophages were transfected with ISD for 2 hours. (C) Whole WT, *Trim21*$^{-/-}$, or *Trim21*$^{-/-}$*Sting1*$^{-/-}$ skin explants were UVB-irradiated as in part C and incubated for 24 hours; (B and C) *Ifnb1* transcript levels were determined via quantitative polymerase chain reaction. All transcript values are relative to unstimulated or transfection reagent-only treated (Lipo) cells. All data represent mean ± SD and are representative of three independent experiments (n = 4 mice per group). Statistical significance was determined using two-way analysis of variance with the Fisher least significant difference test. *$P < 0.05$; **$P < 0.01$; ***$P < 0.001$; ****$P < 0.0001$. In all cases, data representing WT and *Trim21*$^{-/-}$ mice are shown with blue and red bars, and *Trim21*$^{-/-}$*Sting1*$^{-/-}$ is shown with gray. (D) TRIM21 transcript levels were determined in whole blood samples from HCs, SKs, and NSKs. Statistical significance between each group was determined using the uncorrected Dunn test for nonparametric data and is shown on the graph. All data represent mean ± SD, and significance values are given for each analysis. (E) Violin plots comparing the relative expression of *TRIM21* in skin fibroblasts from HCs and CLE skin biopsies (lesional and nonlesional areas) from GSE186476 retrieved and downloaded from GEO. CLE, cutaneous lupus erythematosus; HC, healthy control; ISD, immunostimulatory double-stranded DNA; Lipo, Lipofectamine; NSK, patient with systemic lupus erythematosus with no skin involvement; SK, patient with systemic lupus erythematosus with skin involvement; WT, wild-type.

explants from WT, *Trim21*$^{-/-}$, and *Trim21*$^{-/-}$*Sting*$^{gt/gt}$ mice demonstrated that *Trim21*$^{-/-}$ explants exhibited a STING-dependent increase of *Ifnb1* and *Isg15* expression that could be reversed in the absence of functional STING (Figure 5C; Supplemental Figure 4D). *TRIM21* expression in patients with SLE with documented cutaneous involvement at the time of blood draw was significantly lower in whole blood (Figure 5D) and showed a significant positive correlation with IFI44 (r = 0.48; $P = 1.7^{-6}$), IFI44L (r = 0.44; $P = 1.3^{-5}$), and RSAD2 (r = 0.59; $P = 1.1^{-10}$) (Supplemental Table 2). No significant correlation between TRIM21 and clinical features (kidney involvement; SLEDAI score; or C3, C4, erythrocyte sedimentation rate, and C-reactive protein values) was observed (data not shown). Analysis of *TRIM21* expression in scRNA-seq data from lesional and nonlesional skin biopsies from patients with SLE with cutaneous involvement (GSE186476)[4] showed that *TRIM21* levels were significantly decreased in fibroblasts from lesional and nonlesional skin compared with healthy control skin biopsies (Figure 5D).

Thus, in summary, our data demonstrate that UVB irradiation of murine skin drives IFNβ and ISG expression both locally and systemically in a STING-dependent manner and that the absence of *Trim21* results in exacerbated responses both locally and systemically. The reduction of TRIM21 expression in the whole blood samples of patients with SLE, skin biopsy, and association with cutaneous involvement strengthens our overall hypothesis that TRIM21 acts to restrain systemic IFN responses following environmental triggers, such as UVB exposure of skin.

DISCUSSION

TRIM21 is an important autoantigen associated with cutaneous SLE and is also a critical negative regulator of type I IFN induction in response to RNA and DNA sensing. UVB is an important environmental trigger for cutaneous SLE and in driving systemic flares[1] and has recently been shown in mice to activate both local and systemic type I IFN responses via a cGAS-STING–dependent pathway. This study demonstrates that loss of *Trim21* is associated with enhanced hypersensitivity to UVB exposure, resulting in marked splenomegaly and systemic induction of type I IFNs compared with WT mice. This was accompanied by increased numbers of neutrophils and inflammatory monocytes, both in the circulation and in the spleen, and increased expression of CCR2, a chemokine receptor critical for homing to inflamed tissues (such as the kidney or spleen). Assessing potential targets for TRIM21 in this model revealed that the DNA sensor DDX41 and STING protein levels were stable in *Trim21*$^{-/-}$ murine cells, whereas both were decreased in a time-dependent manner in response to UVB or ISD transfection in cells derived from WT mice. Importantly, enhanced expression of *Ifnb1* in *Trim21*$^{-/-}$ MDFs and BMDMs could be rescued by inhibiting STING signaling. Importantly, we observed decreased expression of TRIM21 in whole blood and skin samples from patients with SLE with cutaneous involvement. Our data underline the importance of TRIM21 as a negative regulator of type I IFN responses and suggest that in the context of UVB-driven responses in SLE, loss of TRIM21 expression or activity may promote UVB-induced SLE exacerbations.

UV irradiation causes damage in cells via direct DNA damage leading to the formation of pyrimidine dimers and activation of the DNA damage response via p53 activation.[6,40] In SLE, UVB exposure is accompanied by type I IFN and CXCL10 induction, which are important in the pathogenesis of cutaneous involvement in SLE.[41] In our studies, absence of *Trim21* results in exacerbated IFNβ and CXCL10 in the skin following UVB exposure, indicating that TRIM21 negatively regulates the production of these cytokines. In addition, we observed enhanced recruitment of CD45+ immune cells, and more importantly, enhanced levels of expression of SIGLEC1, an ISG, on CD11b+ cells, indicating enhanced exposure of these cells to type I IFN. Recent single-cell transcriptomic profiling of cells from lesional and nonlesional skin from patients with SLE with active cutaneous involvement identified an overall high IFN-rich signature in both lesional and nonlesional skin, suggesting that normal-appearing skin in patients with SLE is actually primed immunologically and exists in a prelesional state.[4] These findings suggest that changes in the skin microenvironment promote immune cell infiltration and skewing toward pathogenic subtypes, and here we report that patients with CLE have reduced expression of TRIM21 in both peripheral blood and fibroblasts.

Recent murine studies have shown that, for early responses to UVB, both CCL2 and IFN are required for neutrophil and monocyte recruitment to the skin. In our chronic model of UVB exposure, we observed that inflammatory CD11b^{+}Ly6C^{+} monocytes show increased expression of the chemokine receptor CCR2, the receptor for CCL2 and CXCL10, which is required to home cells to inflamed tissues, including the skin and kidneys.[1,18,19,37,42] Indeed, increased CXCL10 within *Trim21*-deficient kidneys was observed along with increased glomerular cellularity and size and IgG deposition, further supporting the role TRIM21 plays in protecting against systemic inflammation in response to UVB exposure.

Mechanistically, we found that loss of Trim21/TRIM21 in murine or human cells results in enhanced stability of DDX41 and STING in response to cGAS-STING triggers. This is in keeping with similar findings showing that TRIM21 negatively regulates innate immune responses to dsDNA by targeting lysine 9 and lysine 115 on DDX41 for lysine-48(K48)-linked ubiquitination and degradation.[28] Our finding that STING is also stabilized in the absence of TRIM21 suggests a broader role for TRIM21 on the cGAS-STING pathway. One possibility is that TRIM21 destabilizes the interaction between DDX41 and STING in the presence of cGAMP, thus promoting the instability of the complex.[12] However, TRIM21 was recently shown to inhibit radiation-induced mitochondrial DNA (mtDNA) release by promoting the

degradation of VDAC2 via K48-linked ubiquitination and inhibiting type I IFN responses in nasopharyngeal carcinoma.[43] Thus, the potential also exists that in the context of autoimmunity, loss of TRIM21 may result in enhanced mtDNA release and hence exacerbated signaling through the cGAS-STING pathway.

Although TRIM21 is an important autoantigen in SLE and Sjögren disease, its role in the pathobiology of SLE and Sjögren disease has been somewhat ambiguous. As an autoantigen it has been shown to be extruded on blebs of apoptosing keratinocytes in response to UVB irradiation, thus promoting autoantibody formation.[44] It is also an IFN-regulated gene, thus its expression is frequently increased in SLE peripheral immune cells. However, the anomaly of enhanced TRIM21 expression and yet decreased regulation of DNA sensing in SLE immune cells has not been explained to date. This is an important question to tease out as in other forms of inflammatory skin disease, such as psoriasis, TRIM21 reportedly augments inflammation via stabilizing the p65 subunit of nuclear factor κB.[45] How elevated TRIM21 levels in SLE correspond with reduced regulation of cytosolic RNA/DNA sensing is not easily explained. Our previous data showed that TRIM21 needed to be tyrosine phosphorylated to be able to ubiquitinate and target IRF3 for degradation.[46] However, whether activation of TRIM21 is altered in patients with SLE or in the context of skin involvement or UVB sensing is unknown.

Another intriguing possibility was highlighted in a recent publication that showed that patients with SLE had higher expression of TRIM21γ (Ro52γ) isoform.[47] This isoform lacks the SPRY/PRY domain that we and others have shown is important to interact with its downstream targets as we and others have shown, thus making TRIM21γ a potential dominant negative form of TRIM21 that can compete for the E3 ligase machinery and block full-length TRIM21 functions.[22,23,25,29,46] Gomez-Bañuelos et al also suggested it could drive IFNβ induction.[47] Whichever possibility is correct, it suggests that increased levels of TRIM21 can reverse the inhibitory effects of full-length TRIM21 on IFN induction. However, an in-depth analysis of TRIM21 expression and function in SLE patient immune cells and stromal cells is required to fully understand how TRIM21 contributes to autoimmune pathology in the context of SLE. In summary, we have identified a role for TRIM21 as a gatekeeper against UVB-induced systemic disease in mice via its ability to regulate cGAS-STING–dependent signaling at both the local and systemic levels.

AUTHOR CONTRIBUTIONS

All authors contributed to at least one of the following manuscript preparation roles: conceptualization AND/OR methodology, software, investigation, formal analysis, data curation, visualization, and validation AND drafting or reviewing/editing the final draft. As corresponding author, Dr Jefferies confirms that all authors have provided the final approval of the version to be published, and takes responsibility for the affirmations regarding article submission (eg, not under consideration by another journal), the integrity of the data presented, and the statements regarding compliance with institutional review board/Declaration of Helsinki requirements.

REFERENCES

1. Kuechle MK, Elkon KB. Shining light on lupus and UV. Arthritis Res Ther 2007;9(1):101.
2. Sarkar MK, Hile GA, Tsoi LC, et al. Photosensitivity and type I IFN responses in cutaneous lupus are driven by epidermal-derived interferon kappa. Ann Rheum Dis 2018;77(11):1653–1664.
3. Günther C. Nucleic acid immunity in the pathogenesis of cutaneous lupus erythematosus. Front Immunol 2019;10:1636.
4. Billi AC, Ma F, Plazyo O, et al. Nonlesional lupus skin contributes to inflammatory education of myeloid cells and primes for cutaneous inflammation. Sci Transl Med 2022;14(642):eabn2263.
5. Stannard JN, Reed TJ, Myers E, et al. Lupus skin is primed for IL-6 inflammatory responses through a keratinocyte-mediated autocrine type I interferon loop. J Invest Dermatol 2017;137(1):115–122.
6. Svobodová AR, Galandáková A, Sianská J, et al. DNA damage after acute exposure of mice skin to physiological doses of UVB and UVA light. Arch Dermatol Res 2012;304(5):407–412.
7. Collison J. Faulty mitochondrial DNA repair promotes inflammation in RA. Nat Rev Rheumatol 2019;15(10):576.
8. Barber GN. STING-dependent cytosolic DNA sensing pathways. Trends Immunol 2014;35(2):88–93.
9. Hagiwara AM, Moore RE, Wallace DJ, et al. Regulation of cGAS-STING pathway - implications for systemic lupus erythematosus. Rheumatol Immunol Res 2021;2(3):173–184.
10. McWhirter SM, Jefferies CA. Nucleic acid sensors as therapeutic targets for human disease. Immunity 2020;53(1):78–97.
11. Parvatiyar K, Zhang Z, Teles RM, et al. The helicase DDX41 recognizes the bacterial secondary messengers cyclic di-GMP and cyclic di-AMP to activate a type I interferon immune response. Nat Immunol 2012;13(12):1155–1161.
12. Zhang Z, Yuan B, Bao M, et al. The helicase DDX41 senses intracellular DNA mediated by the adaptor STING in dendritic cells. Nat Immunol 2011;12(10):959–965.
13. Sun L, Wu J, Du F, et al. Cyclic GMP-AMP synthase is a cytosolic DNA sensor that activates the type I interferon pathway. Science 2013;339(6121):786–791.
14. Ablasser A, Goldeck M, Cavlar T, et al. cGAS produces a 2′-5′-linked cyclic dinucleotide second messenger that activates STING. Nature 2013;498(7454):380–384.
15. Gao D, Wu J, Wu YT, et al. Cyclic GMP-AMP synthase is an innate immune sensor of HIV and other retroviruses. Science 2013;341(6148):903–906.
16. Wu J, Sun L, Chen X, et al. Cyclic GMP-AMP is an endogenous second messenger in innate immune signaling by cytosolic DNA. Science 2013;339(6121):826–830.
17. Diner EJ, Burdette DL, Wilson SC, et al. The innate immune DNA sensor cGAS produces a noncanonical cyclic dinucleotide that activates human STING. Cell Rep 2013;3(5):1355–1361.
18. Skopelja-Gardner S, An J, Tai J, et al. The early local and systemic type I interferon responses to ultraviolet B light exposure are cGAS dependent. Sci Rep 2020;10(1):7908.
19. Sontheimer C, Liggitt D, Elkon KB. Ultraviolet B irradiation causes stimulator of interferon genes-dependent production of protective type I interferon in mouse skin by recruited inflammatory monocytes. Arthritis Rheumatol 2017;69(4):826–836.
20. Oke V, Vassilaki I, Espinosa A, et al. High Ro52 expression in spontaneous and UV-induced cutaneous inflammation. J Invest Dermatol 2009;129(8):2000–2010.

21. Arimoto KI, Miyauchi S, Stoner SA, et al. Negative regulation of type I IFN signaling. J Leukoc Biol 2018;103(6):1099–1116.
22. Higgs R, Lazzari E, Wynne C, et al. Self protection from anti-viral responses--Ro52 promotes degradation of the transcription factor IRF7 downstream of the viral Toll-Like receptors. PLoS One 2010; 5(7):e11776.
23. Higgs R, Ní Gabhann J, Ben Larbi N, et al. The E3 ubiquitin ligase Ro52 negatively regulates IFN-beta production post-pathogen recognition by polyubiquitin-mediated degradation of IRF3. J Immunol 2008;181(3):1780–1786.
24. Lazzari E, Korczeniewska J, Ní Gabhann J, et al. TRIpartite motif 21 (TRIM21) differentially regulates the stability of interferon regulatory factor 5 (IRF5) isoforms. PLoS One 2014;9(8):e103609.
25. Espinosa A, Dardalhon V, Brauner S, et al. Loss of the lupus autoantigen Ro52/Trim21 induces tissue inflammation and systemic autoimmunity by disregulating the IL-23-Th17 pathway. J Exp Med 2009; 206(8):1661–1671.
26. Yang B, Wang J, Sun B. Trim21: a novel negative regulator in DNA sensor signaling. Cell Mol Immunol 2013;10(3):190–192.
27. Yoshimi R, Ishigatsubo Y, Ozato K. Autoantigen TRIM21/Ro52 as a possible target for treatment of systemic lupus erythematosus. Int J Rheumatol 2012;2012:718237.
28. Zhang Z, Bao M, Lu N, et al. The E3 ubiquitin ligase TRIM21 negatively regulates the innate immune response to intracellular double-stranded DNA. Nat Immunol 2013;14(2):172–178.
29. Jefferies C, Wynne C, Higgs R. Antiviral TRIMs: friend or foe in autoimmune and autoinflammatory disease? Nat Rev Immunol 2011;11(9): 617–625.
30. Wu T, Hu E, Xu S, et al. clusterProfiler 4.0: a universal enrichment tool for interpreting omics data. Innovation (Camb) 2021;2(3):100141.
31. Ulgen E, Ozisik O, Sezerman OU. pathfindR: an R package for comprehensive identification of enriched pathways in omics data through active subnetworks. Front Genet 2019;10:858.
32. Butler A, Hoffman P, Smibert P, et al. Integrating single-cell transcriptomic data across different conditions, technologies, and species. Nat Biotechnol 2018;36(5):411–420.
33. Toda G, Yamauchi T, Kadowaki T, et al. Preparation and culture of bone marrow-derived macrophages from mice for functional analysis. STAR Protoc 2020;2(1):100246.
34. Khan M, Gasser S. Generating primary fibroblast cultures from mouse ear and tail tissues. J Vis Exp 2016;(107):53565.
35. Mazzalupo S, Wawersik MJ, Coulombe PA. An ex vivo assay to assess the potential of skin keratinocytes for wound epithelialization. J Invest Dermatol 2002;118(5):866–870.
36. Gehrke N, Mertens C, Zillinger T, et al. Oxidative damage of DNA confers resistance to cytosolic nuclease TREX1 degradation and potentiates STING-dependent immune sensing. Immunity 2013;39(3): 482–495.
37. Skopelja-Gardner S, Tai J, Sun X, et al. Acute skin exposure to ultraviolet light triggers neutrophil-mediated kidney inflammation. Proc Natl Acad Sci USA 2021;118(3):e2019097118.
38. Sauer JD, Sotelo-Troha K, von Moltke J, et al. The N-ethyl-N-nitrosourea-induced Goldenticket mouse mutant reveals an essential function of Sting in the in vivo interferon response to Listeria monocytogenes and cyclic dinucleotides. Infect Immun 2011;79(2):688–694.
39. Haag SM, Gulen MF, Reymond L, et al. Targeting STING with covalent small-molecule inhibitors. Nature 2018;559(7713):269–273.
40. Besaratinia A, Synold TW, Chen HH, et al. DNA lesions induced by UV A1 and B radiation in human cells: comparative analyses in the overall genome and in the p53 tumor suppressor gene. Proc Natl Acad Sci USA 2005;102(29):10058–10063.
41. Erazo-Martínez V, Tobón GJ, Cañas CA. Circulating and skin biopsy-present cytokines related to the pathogenesis of cutaneous lupus erythematosus. Autoimmun Rev 2023;22(2):103262.
42. Boring L, Gosling J, Chensue SW, et al. Impaired monocyte migration and reduced type 1 (Th1) cytokine responses in C-C chemokine receptor 2 knockout mice. J Clin Invest 1997;100(10):2552–2561.
43. Li JY, Zhao Y, Gong S, et al. TRIM21 inhibits irradiation-induced mitochondrial DNA release and impairs antitumour immunity in nasopharyngeal carcinoma tumour models. Nat Commun 2023;14(1):865.
44. Saegusa J, Kawano S, Koshiba M, et al. Oxidative stress mediates cell surface expression of SS-A/Ro antigen on keratinocytes. Free Radic Biol Med 2002;32(10):1006–1016.
45. Yang L, Zhang T, Zhang C, et al. Upregulated E3 ligase tripartite motif-containing protein 21 in psoriatic epidermis ubiquitylates nuclear factor-κB p65 subunit and promotes inflammation in keratinocytes. Br J Dermatol 2021;184(1):111–122.
46. Stacey KB, Breen E, Jefferies CA. Tyrosine phosphorylation of the E3 ubiquitin ligase TRIM21 positively regulates interaction with IRF3 and hence TRIM21 activity. PLoS One 2012;7(3):e34041.
47. Gomez-Bañuelos E, Wahadat MJ, Li J, et al. Alternative exon usage in TRIM21 determines the antigenicity of Ro52/TRIM21 in systemic lupus erythematosus. JCI Insight 2022;7(19):e163795.